

Defects at the Si(111)/SiO₂ interface investigated with low-energy electron diffraction

J. Wollschläger and M. Henzler

Institut für Festkörperphysik, Universität Hannover, Appelstrasse 2, 3000 Hannover 1, Federal Republic of Germany

(Received 5 October 1988)

After removal of the oxide, defects at the Si/SiO₂ interface have been studied by a high-resolution low-energy-electron-diffraction (HR-LEED) system. Analyzing the profile of LEED spots, we are able to detect two different kinds of defects, one due to steps and the other due to inhomogeneities. The HR-LEED measurements enable us to determine the terrace length distribution and the size distribution of inhomogeneities with atomic resolution. Both are described by a geometric distribution. The investigated samples with a thin oxide layer (10 nm, dry oxidation) are characterized by very low step densities at the interface. The boundary between the silicon crystal and its oxide is extremely sharp; within the transfer width of the instrument (~ 70 nm) the interface changes between only two silicon layers. Therefore, annealing cannot drastically improve the quality of the interface. On the other side there are many inhomogeneities in small patches. In contrast to the steps, they are drastically reduced by annealing of the wafers.

I. INTRODUCTION

The development of semiconductor devices integrated on a large scale requires the production of very thin oxides. Because the interfaces of these thin oxides are very close to the initial silicon surface before oxidation, influences of the processes before, during, and after the oxidation are very important for the quality of both the final oxide and its interface to the silicon.

The quality of metal-oxide semiconductor (MOS) devices is strongly affected by the quality of the oxide because the carriers in the inversion layer are very close to the Si/SiO₂ interface. Scattering of the electrons by fixed charges, surface states, and interface roughness are believed to be the major contributions to the mobility, especially at low temperatures.¹⁻³ Numerous investigations have been concentrated on chemistry and electrical properties of the Si/SiO₂ interface whereas, first, the structural properties have been neglected due to the lack of appropriate measuring techniques. In the meantime, several techniques with atomic resolution have been developed and applied to interface studies: transmission electron microscopy (TEM), scanning tunnel microscopy (STM), x-ray photoemission spectroscopy (XPS), x-ray diffraction, and low-energy electron diffraction (LEED) provide information on defects, especially atomic steps at the interface.^{4,5}

For XPS the oxide is chemically thinned to less than the escape depth of the photoelectrons. The number of steps and other defects is indirectly concluded out of the density of different charged silicon atoms determined by the chemical shift of the silicon *2p* electrons.⁶⁻⁹ Cross sections of wafers are prepared by grinding and ion milling to produce images with an atomic resolution by the electron beam of the TEM parallel to the interface. These images, which show directly the profile of the interface with the oxide in place, are digitized to analyze quantitatively the interface roughness.¹⁰⁻¹² For LEED

the oxide is completely removed to provide a diffraction pattern of the bare silicon crystal. The roughness of the interface gives rise to a broadening of the diffracted electron beam. The roughness is determined quantitatively by the spot-profile analysis (SPA-LEED).¹³⁻¹⁵ So far there are only preliminary investigations by STM (Ref. 16) and x-ray diffraction.¹⁷

In the present paper, we investigate the influence of annealing on the defects of the Si(111)/SiO₂ interface. For this purpose we have used spot-profile analysis of the electron beam diffracted by the interface after removal of the oxide. For the first time we have surveyed spots for many electron energies by a high-resolution LEED system. The broadenings of the spots are split into two shoulders which behave very differently, changing the energy of the electron beam. This can only be explained by defects at the interface due to both steps and inhomogeneities. The analysis of the spot profiles provide us detailed information about the healing of defects at the interface by annealing.

II. EVALUATION OF SPOT PROFILES

An overview of the influence of defects at surfaces on spot profiles is reported in Refs. 4 and 18. The evaluation of spot profiles is described in full detail by these reports and the literature cited herein. Further aspects concerning the scattering by inhomogeneities are addressed in Ref. 19. Here we will only briefly recapitulate the main features of the theory necessary to analyze the LEED investigations of the Si(111)/SiO₂ interface reported here.

The surface of the crystal may be described by the positions \mathbf{r}_n of the surface atoms possessing the scattering amplitude f_n . We assume that all atoms are on perfect lattice sites $\mathbf{r}_n = \mathbf{a}\mathbf{n} + dh(\mathbf{n})\mathbf{e}_1$, where $\mathbf{a}\mathbf{n}$ and $dh(\mathbf{n})\mathbf{e}_1$ are the lateral and vertical components of \mathbf{r}_n , respectively, in integer multiples of the lateral lattice constant a and the

layer spacing d , respectively. The intensity of the diffracted electron beam is

$$I(\mathbf{K}, \mathbf{k}_i) = \sum_{\mathbf{n}, \mathbf{m}} f_{\mathbf{n}} f_{\mathbf{m}}^* \exp\{idK_{\perp}[h(\mathbf{n}) - h(\mathbf{m})]\} \times \exp[ia\mathbf{K}_{\parallel}(\mathbf{n} - \mathbf{m})], \quad (1)$$

where \mathbf{K}_{\parallel} and K_{\perp} denote the components of the scattering vector $\mathbf{K} = \mathbf{k}_i - \mathbf{k}_f$ parallel and perpendicular to the surface, respectively, while \mathbf{k}_i and \mathbf{k}_f are the wave vectors of the incoming and the scattered electron, respectively.

Equation (1) is exact, but it is not easy to operate with it. To obtain a much more usable expression, which includes effects caused by inhomogeneities at the surface, we consider only two different kinds of scatterers with amplitudes f_A and f_B , whose distribution is not affected by surface roughness. This assumption enables us to rearrange Eq. (1), considering separately inhomogeneities and surface roughness, so that we obtain (for details, see Ref. 19)

$$I(\mathbf{K}, \mathbf{k}_i) = |\langle f \rangle|^2 G(\mathbf{K}) + \Theta_A \Theta_B |\Delta f|^2 G(\mathbf{K}) * \Phi_{\text{inh}}(\mathbf{K}_{\parallel}). \quad (2)$$

Here, Θ_A and Θ_B denote the coverage of type A and B , respectively, and the asterisk denotes the convolution. $\langle f \rangle$ is the average scattering amplitude $\langle f \rangle = \Theta_A f_A + \Theta_B f_B$, while Δf denotes their difference $\Delta f = f_A - f_B$. $\Phi_{\text{inh}}(\mathbf{K}_{\parallel})$ is the broadening of the spot profile due to inhomogeneities and $G(\mathbf{K})$ the lattice factor

$$G(\mathbf{K}) = \sum_{\mathbf{n}, \mathbf{m}} \exp\{idK_{\perp}[h(\mathbf{n}) - h(\mathbf{m})]\} \exp[ia\mathbf{K}_{\parallel}(\mathbf{n} - \mathbf{m})], \quad (3)$$

which includes all information about the surface roughness. It is the Fourier transform of the pair correlation of the surface $C(\mathbf{r})$ defined as the probability to find two surface atoms separately by a distance \mathbf{r} .

If there is no inhomogeneity at the surface the second term of Eq. (2) vanishes. Therefore the spot profile of an electron beam diffracted at a homogeneous surface is only influenced by the surface roughness, especially steps. As has been reported earlier, random steps at the surface split the spot profile into a central spike and a broadening.^{4,18} This is a consequence of an equivalent splitting of the lattice factor into a sharp δ -function spike and a shoulder. Both spike and shoulder vary in intensity with K_{\perp} periodically. The variation of the central spike $G_0(K_{\perp})$ is used to evaluate the layer distribution.^{20,21}

Close to the in-phase condition $dK_{\perp} = 2\pi m$ (m denotes an integer), the variation of the central spike $G_0(K_{\perp})$ is not determined by the details of the layer distribution. It is influenced only by the asperity height Δ of the surface (rms deviation from the average surface¹⁹). The leading terms of the Taylor expansion of the variation $G_0(K_{\perp})$ close to the in-phase condition are

$$G_0(K_{\perp}) = 1 - \Delta^2 (\delta K_{\perp})^2. \quad (4)$$

Here ΔK_{\perp} denotes the deviation of the vertical component K_{\perp} from the in-phase condition. Thus the variation of the central spike close to the in-phase condition enables us to determine the asperity height of the surface without using any other parameter.

On the other side, the terrace distribution may be derived from the shape of the shoulder.^{22,23} Roughly speaking, the half-width of the broadening behaves reciprocally to the average terrace length.

Considering a one-dimensional surface, several methods have been reported to calculate the lattice factor given any terrace length distribution.^{15,23} In particular, a two-level surface has been considered: substrate ($i=0$) plus one adlayer ($i=1$).²⁴ Assuming that both layers are governed by a geometric distribution $P_i(\Gamma)$ for the probability of finding a terrace length Γ ,

$$P_i(\Gamma) = \gamma_i (1 - \gamma_i)^{\Gamma/a - 1}, \quad (5)$$

where a/γ_i denotes the average terrace length $\langle \Gamma \rangle_i$ for each layer, the lattice factor is

$$G(\mathbf{K}) = [\Theta_0^2 + \Theta_1^2 + 2\Theta_0\Theta_1 \cos(dK_{\perp})] \sum_{\mathbf{m}} \delta(a\mathbf{K}_{\parallel} - 2\pi\mathbf{m}) + 2\Theta_0\Theta_1 \cos(dK_{\perp}) \frac{(1 - \beta_{\text{step}}^2)/2\pi}{1 + \beta_{\text{step}}^2 - 2\beta_{\text{step}} \cos(a\mathbf{K}_{\parallel})}. \quad (6)$$

Here Θ_0 and Θ_1 denote the coverage of substrate and adlayer, respectively. It should be remarked that the broadening behaves like a Lorentzian close to the center of the Brillouin zone. The parameter β_{step} involved in the broadening is related to the average terrace length via $\beta_{\text{step}} = 1 - \gamma_0 - \gamma_1$. This lattice factor implies that the pair correlation of the surface $C(\mathbf{r})$ approaches exponentially its value at infinity. The correlation length of the surface roughness L_{step} governing the decay of the autocorrelation is also related to the parameter β_{step} via $\beta_{\text{step}} = \exp(-a/L_{\text{step}})$. If the average terrace lengths are not too small, we can approximate the correlation length by the relation $a/L_{\text{step}} = \gamma_0 + \gamma_1$.

Equation (2) shows that the inhomogeneity of the surface produces additional broadenings of the spot via the convolution of the lattice factor and the additional broadening $\Phi_{\text{inh}}(\mathbf{K}_{\parallel})$ due to inhomogeneities. If the broadening due to steps is sufficiently small, the convolution of the lattice factor with $\Phi_{\text{inh}}(\mathbf{K}_{\parallel})$ does not change $\Phi_{\text{inh}}(\mathbf{K}_{\parallel})$. Thus, there is only one additional broadening, which depends only on K_{\perp} via the scattering amplitudes.

Similar to the roughness model of Ref. 24, we consider a one-dimensional model of the surface. The distributions $P_i(\Lambda)$ of domain sizes Λ possessing the same scattering amplitude of type A or B , denoted by i , are supposed to be geometric ones:

$$P_i(\Lambda) = \lambda_i (1 - \lambda_i)^{\Lambda/a - 1}, \quad (7)$$

where a/λ_i is the average domain size $\langle \Lambda \rangle_i$. Naturally, this model also predicts that the correlation of surface inhomogeneity goes exponentially to its value at infinity (see also Ref. 19). Similar to the correlation length of sur-

face roughness L_{step} we define the correlation length of surface inhomogeneity L_{inh} , which is related to the average domain size by $\exp(-a/L_{\text{inh}}) = 1 - \lambda_A - \lambda_B$, which may be approximated by $a/L_{\text{inh}} = \lambda_A + \lambda_B$, if the average domain sizes of both kinds of scatterers are not too small. The exponential behavior of the correlation again results in a Lorentzian-like shape of the broadening:

$$\Phi_{\text{inh}}(K_{\perp}) = \frac{(1 - \beta_{\text{inh}}^2)/2\pi}{1 + \beta_{\text{inh}}^2 - 2\beta_{\text{inh}} \cos(aK_{\parallel})}, \quad (8)$$

where the parameter β_{inh} is defined by $\beta_{\text{inh}} = \exp(-a/L_{\text{inh}})$. This result shows that a geometric distribution of inhomogeneities brings about the same shape of broadening as a geometric distribution of terraces. There is a great difference, however, between both kinds of broadenings. While the broadening due to roughness vanishes generally at the in-phase condition, the broadening due to inhomogeneity may still remain. This enables us to distinguish between both kinds of defects by analyzing spot profiles for many energies of the electron beam.

III. EXPERIMENTAL METHOD

At a temperature of 800 °C commercially polished silicon (111) wafers have been oxidized in dry oxygen until a 10-nm-thick oxide has been grown. The wafers were annealed in a nitrogen atmosphere at 800 or 1000 °C for different times.

Since the electron beam cannot penetrate the oxide, it is necessary to remove the oxide without damage to the substrate to study the morphology of the Si/SiO₂ interface of the wafers by a HR-LEED system in an ultrahigh-vacuum (UHV) chamber. For that purpose the oxidized samples were etched in a HF solution. During the transfer into the UHV chamber the samples were covered by methanol to protect them against reoxidation (for details, see Refs. 13 and 14). Since the pressure after transfer of a sample again decreases to values lower than 1×10^{-8} Pa, the LEED intensities and profiles did not change during hours of measurement.

The HR-LEED system consists of an electron gun and a detector at a fixed position in backward-scattering direction. The spot profile of the backscattered electron beam has been scanned by an electrostatic deflection system. Therefore, no mechanical movement of the sample has been necessary. The electron beam has been focused onto the detector by a magnetic lens. A transfer width of 70 nm has been achieved by this system.²⁵

IV. RESULTS

Spot profiles have been measured along the reciprocal lattice (00) rod between the (555) and the (666) Bragg reflexes, so that the phase S , defined by $2\pi S = dK_{\perp}$, has been varied between 5 and 6. For the out-of-phase condition ($S = 5.5$), Fig. 1 shows the profile of a wafer immediately after transfer. This shape of the profile is typical for all samples. For comparison purposes, Fig. 1(a) also shows the profile produced by a wafer well annealed in UHV (solid line), which reproduces the instrumental

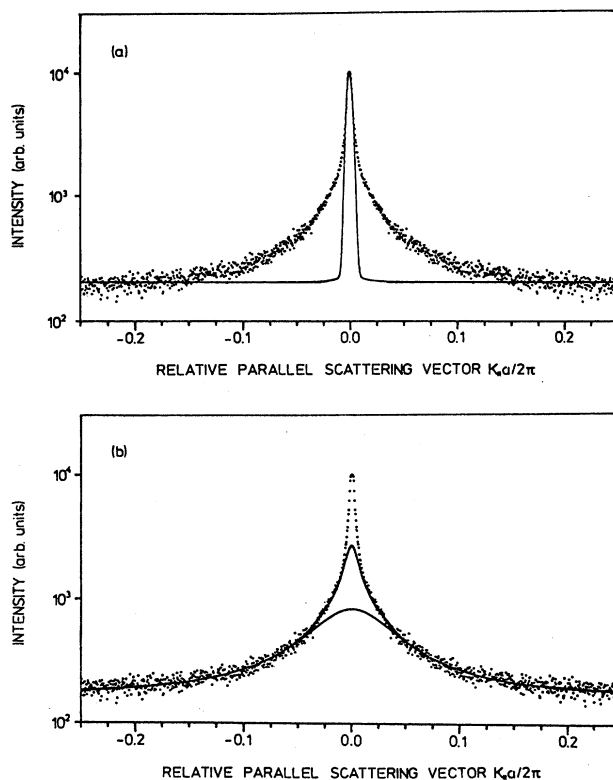


FIG. 1. The spot profile of the (00) beam for an unannealed wafer at the out-of-phase condition (115 eV). (a) For comparison, the spot profile of a well-annealed wafer is shown as a solid line (instrumental response). (b) The solid line shows the fit of the broadening to the sum of two Lorentzian-like shoulders (lower curve, broad shoulder; upper curve, sum of both shoulders). Please notice the logarithmic scale of the ordinate. The abscissa is relative to the next normal spot position.

broadening. The difference between both curves is the broadening due to defects. It is easy to separate crystal spike, broadening, and constant background intensity. The solid line of Fig. 1(b) illustrates that the broadening is fitted well by the sum of two Lorentzian-like shoulders described by Eqs. (6) and (8). Therefore, all measured profiles have been submitted to a least-squares fit to the sum of a δ spike convoluted by the instrumental broadening, two Lorentzian-like shoulders, and a constant background. Please notice the logarithmic scale in Fig. 1.

Since the constant background is caused by thermal diffuse scattering or randomly distributed point defects, it will not be considered here further. On the other hand, the three other components are studied carefully for many energies of the electron beam. The analysis shows that the half-widths of both broadenings do not depend on the phase S , but their amplitudes vary considerably. Naturally, this means that the integrated intensities of all parts of the spot profiles depend on the phase S .

Another very interesting feature of the measured profiles is shown in Fig. 2. We can clearly see from it that the measured profile for the in-phase condition ($S = 6.0$) is not completely described by a central spike,

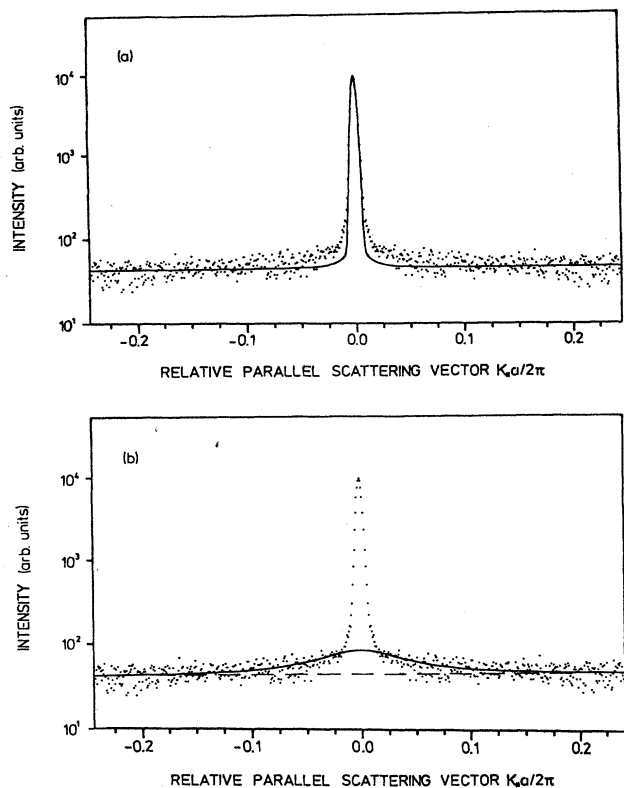


FIG. 2. The spot profile of the (00) beam for the same wafer as in Fig. 1 at the in-phase-condition $S=6.0$ (137 eV). (a) The solid line (instrumental response) shows that an additional broadening not due to steps has to be considered. (b) The additional broadening is fitted well by a Lorentzian-like shoulder of the same half-width as the broad shoulder at the out-of-phase condition (solid line). The dashed line is the constant background.

as would be expected supposing that steps are the only defects at the surface. On the contrary, there still remains a broadening which can be identified as the broad shoulder also observed at other energies. Thus we conclude that the narrow shoulder is due to steps and the broad one due to inhomogeneities.

Changing the phase S from 5.0 to 6.0, the two parts of the diffuse intensity behave very differently. The ratio of the integrated intensity of the broad shoulder to the total intensity G_{inh} is nearly constant, except a small range near $S=5.5$. On the other hand, the ratio of the integrated intensity of the narrow shoulder to the total intensity G_{step} behaves sinusoidally except in the range where G_{inh} also differs significantly from constancy. Figure 3 demonstrates that these ratios are almost the same for all samples except scaling. These different behaviors of both broadenings is an additional hint that the narrow shoulder is caused by surface roughness while the broad one is due to inhomogeneities at the surface.

All these features of the LEED investigations may be explained by the model described in Sec. II. There exists one broadening due to surface roughness and one due to inhomogeneity. Since the half-width of the broadening

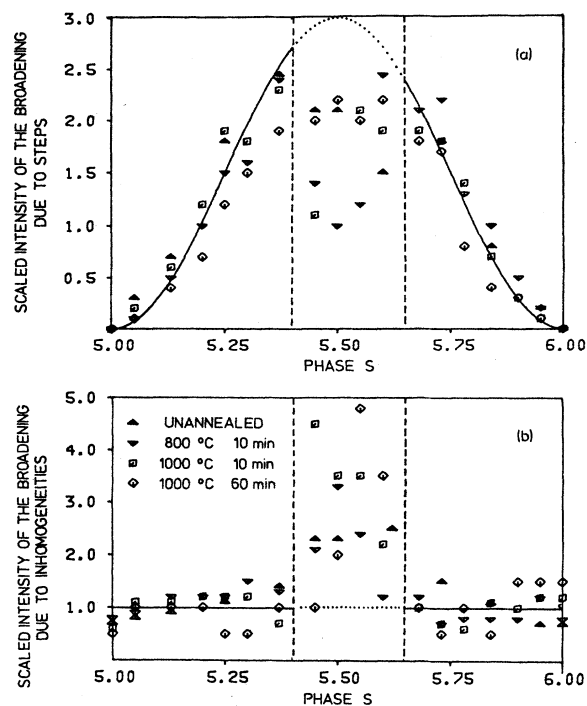


FIG. 3. The phase variation of the intensity in the shoulders. (a) The ratio G_{step} of the integrated intensity of the narrow shoulder to the total intensity. The curves are scaled with respect to their values close to $S=5.25$ and 6.75 . (b) The ratio G_{inh} of the integrated intensity of the broad shoulder to the total intensity. The curves are scaled with their value close to the in-phase conditions $S=5.0$ and 6.0 . The solid line illustrates that the approximation that the scattering amplitudes differ drastically is valid for nearly the whole range of the vertical phase S . There are only deviations from the theoretically predicted curves within a small range close to the out-of-phase condition signed by the dashed lines.

caused by inhomogeneity is much larger than the half-width of the broadening due to steps, the shape of the broad shoulder is not noticeably changed by the convolution with the lattice factor. Therefore, only one additional broadening may be observed. Following Eq. (2) we will consider at first the central spike and the narrow shoulder to analyze the surface roughness. Then we will make use of the broad shoulder to obtain information about the inhomogeneity.

The variation of the central spike with respect to the phase $G_0(S)$ indicates that the interface of all samples may be described well by a two-level system. The coverages of the substrate and adlayer have been evaluated by fitting the experimental data to the theoretically predicted variation shown by Eq. (6) (see Fig. 4). Since LEED cannot distinguish between Θ_1 and $1-\Theta_1$, we have chosen $\Theta_1 \leq 0.5$ for convenience. The asperity height of the interface, which does not have the ambiguity of the coverage, has been analyzed by a plot of the data close to the in-phase conditions $S=5.0$ and 6.0 versus the phase S . For practical reasons (see also Ref. 19) we have not used the parabolic approximation of Eq. (5) but

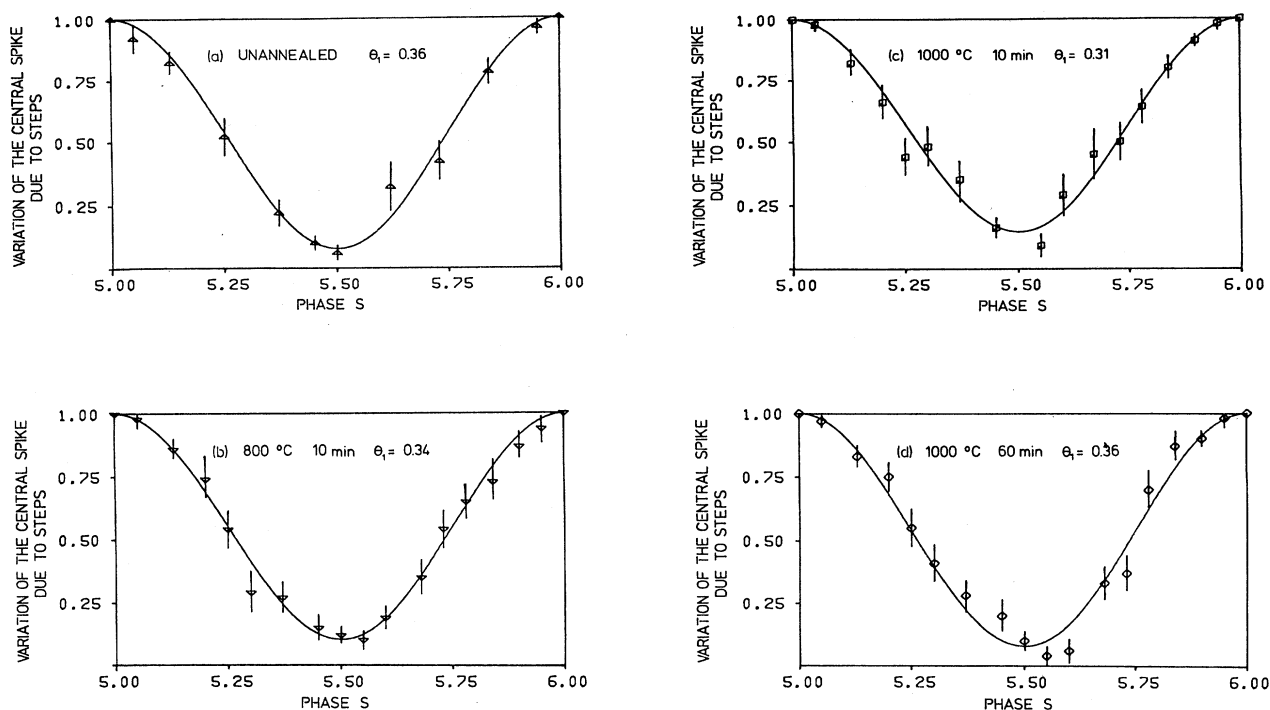


FIG. 4. The lattice factor due to steps G_0 (integrated intensity of central spike over sum of central spike and narrow shoulder). The solid line shows the theoretically predicted dependence for a two-level system fitted solely with the coverage Θ_1 of the adlayer. (a) The unannealed wafer, (b) the wafer annealed at 800°C for 10 min, (c) the wafer annealed at 1000°C for 10 min, and (d) the wafer annealed at 1000°C for 60 min.

instead have used the Gaussian approximation $G_0 = \exp[-\Delta^2(\delta K_{\perp})^2]$ to get a better fit also for phases not too close to the in-phase condition (see Fig. 5). Both coverages and asperity heights obtained by this analysis are shown in Table I.

The Lorentzian-like shape of the broadening may be explained by a geometric terrace length distribution. As has been mentioned earlier, the parameter β_{step} has been calculated by a least-squares fit of the measured narrow shoulder to the shoulder theoretically predicted by Eq. (7). The correlation length of surface roughness $L_{\text{step}} = -a/\ln(\beta_{\text{step}})$ determined by these fits is also shown in Table I. According to the one-dimensional model we ob-

tain the average terrace length of each layer for a cross section of the surface by considering the relation $\Theta_0/\langle\Gamma\rangle_0 = \Theta_1/\langle\Gamma\rangle_1$ and the parameter β_{step} .^{24,26} This enables us to calculate the average terrace lengths and the step-atom densities for a cross section as shown in Table I. The step-atom density for a cross section is half the step-atom density of the surface supposing that the terraces are arranged with parallel edges. Otherwise, the details of the two-dimensional arrangement produce an additional factor in order of magnitude of 1.

We now continue by analyzing the broad shoulder. The constancy of G_{inh} for a wide range of the phase S implies that one of the scattering amplitudes is much small-

TABLE I. The steps at the interface.

Post treatment of the Si(111)/SiO ₂ interface	Θ_0 (% of ML)	Θ_1 (% of ML)	$\langle\Gamma\rangle_0$ (nm)	$\langle\Gamma\rangle_1$ (nm)	Step atoms per surface atom for a cross section ($\times 10^{-2}$)	Step atoms per surface atoms ($\times 10^{-2}$)	Step atom density ($\times 10^{17} \text{ m}^{-2}$)	Δ (Å)	L_{step} (nm)
None	64±6	36±6	19±5	10±2	2.3±0.4	4.6±0.8	2.8±0.5	1.51 ±0.06	6.5±0.7
800 °C 10 min	66±7	34±7	20±6	10±2	2.2±0.4	4.4±0.8	2.6±0.5	1.48 ±0.06	6.5±0.7
1000 °C 10 min	69±11	31±11	22±10	10±3	2.1±0.6	4.2±1.2	2.5±0.7	1.44 ±0.16	6.5±0.7
1000 °C 60 min	64±5	36±5	19±4	10±2	2.3±0.4	4.6±0.8	2.8±0.5	1.51 ±0.03	6.5±0.7

TABLE II. The inhomogeneities of the surface.

Post treatment of the Si(111)/SiO ₂ interface	Θ_{Si} (% of ML)	Θ_{inh} (% of ML)	$\langle \Lambda \rangle_{\text{Si}}$ (nm)	$\langle \Lambda \rangle_{\text{inh}}$ (nm)	Inhom. per surface atom for a cross section ($\times 10^{-2}$)	Inhom. per surface atom ($\times 10^{-4}$)	Density of inhom. ($\times 10^{15} \text{ m}^{-2}$)	L_{inh} (nm)
None	87±2	13±2	10±2	1.5±0.1	2.8±0.5	7.8±2.8	4.7±1.7	1.16±0.05
800°C 10 min	76±5	24±5	6±2	1.8±0.2	4.1±0.8	16.8±6.6	10.1±4.0	1.34±0.07
1000°C 10 min	85±5	15±5	14±5	2.5±0.3	2.0±0.7	4.0±2.8	2.4±1.7	1.91±0.13
1000°C 60 min	95±2	5±2	57±27	2.9±0.3	0.6±0.2	0.66±0.24	0.22±0.14	2.60±0.23

er than the other one, because by using this assumption the ratio of $\langle f \rangle$ to Δf is constant. G_{inh} increases drastically only close to $S=5.5$. Here the $I(V)$ curve of the Si(111) has a minimum of intensity, which means that here the scattering amplitude f_{Si} of the silicon is minimal. Thus we conclude that the scattering amplitude f_{inh} of the second unknown kind of scatterers is much smaller than that of the silicon for most energies. With this approximation $f_{\text{inh}} \ll f_{\text{Si}}$ we obtain the total intensity $I_{\text{tot}} = \Theta_{\text{Si}} |f_{\text{Si}}|^2$, while the integrated intensity of the broad shoulder is $I_{\text{inh}} = \Theta_{\text{Si}} (1 - \Theta_{\text{Si}}) |f_{\text{Si}}|^2$. Thus the fraction of the total intensity in the broad shoulder G_{inh} in the range of $f_{\text{inh}} \ll f_{\text{Si}}$ is $G_{\text{inh}} = 1 - \Theta_{\text{Si}} = \Theta_{\text{inh}}$ and is therefore used directly to determine the coverage Θ_{inh} of inhomogeneities (see Table II).

Also, here the Lorentzian-like shape of the broad shoulder indicates that the domain sizes are geometrically distributed. Therefore, the evaluation of the average domain size for a cross section of the surface is very similar to that of the average terrace length for a cross section (see also Sec. II). The correlation lengths of the inhomogeneity and the average domain sizes of the silicon areas and the second unknown species are shown in Table

II. Furthermore, Table II shows the number of inhomogeneity domains per surface atoms of a cross section. To obtain the total number of inhomogeneities per surface atom we suppose that the inhomogeneities are also distributed in parallel rows. But contrary to the step-atom density, this assumption implies that the density of inhomogeneities is the square of the densities for a cross section. Thus, as Table II illustrates, the inhomogeneities are reduced drastically by annealing: the unannealed wafer has 4.7×10^{15} inhomogeneities per m^2 , while the wafer annealed in nitrogen for 1 h at 1000°C shows only 2.2×10^{14} inhomogeneities per m^2 .

V. DISCUSSION

The analysis of the spot profile of the electron beam diffracted by the Si(111)/SiO₂ interface reported in Sec. IV demonstrates that SPA-LEED is a powerful tool for examining the interface and determining a lot of details of its morphology. For the first time we are able to distinguish between two different kinds of broadening caused by steps at the interface and its inhomogeneity, respectively, by measuring profiles for many energies of the electrons over a wide range of the surface Brillouin zone and by an appropriate scaling with the total integrated intensity.

Now the energy variation of the central spike allows us to determine the asperity height and the layer distribution beyond the step-atom density and the terrace length distribution investigated earlier by LEED.^{13,14,27} The observed interface roughness of all samples is extremely low. The step-atom density of the unannealed wafer is still 5–10 times lower than the density previously reported. Also, the analysis of the vertical roughness shows a sharp boundary between the silicon crystal and its oxide: within the transfer width of the high-resolution instrument the sharp interface varies only between two levels. This result agrees with the asperity height investigated by TEM.³

Since Goodnick *et al.*³ have used the autocovariance of the interface to characterize its roughness, we are not able to compare directly the terrace length distribution we have evaluated with their data. But we have shown elsewhere¹⁹ that, close to the in-phase condition, the shoulder caused by interface roughness has the shape of the Fourier transform of the autocovariance. Therefore,

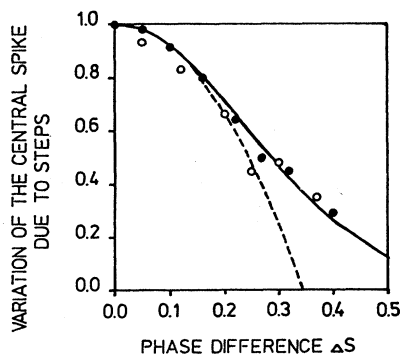


FIG. 5. The modulation of the central spike close to the in-phase conditions $S=5.0$ (open symbols) and $S=6.0$ (solid symbols). The solid line is a fit to the Gaussian approximation and the dashed line the second-order Taylor expansion. For both curves we have used the asperity height $\Delta=1.44 \text{ \AA}$ also obtained by a fit to the theoretically predicted variation of the central spike due to roughness for a two-level surface [see Fig. 4(c)]. The wafer was annealed at 1000°C for 10 min.

the Lorentzian-like shape of the broadenings due to steps implies an exponential behavior of the autocovariance, as has been reported previously in Ref. 3. These results are not compatible with the Gaussian approximation for the autocovariance widely used to describe the mobility of the two-dimensional electron gas of metal-oxide semiconductor transistors.¹⁻³ But, agreeing with the extremely low step density observed at all samples, the correlation length of the examined interface is much longer than that reported by the TEM investigations.

An exceptional feature of the profile analysis, which we have observed for the first time, is the additional nearly-energy-independent broad shoulder which can be explained by a second type of species in domains with different scattering amplitudes. There may be mainly two reasons that such a broadening has not been reported so far. The amplitude of the broad shoulder is extremely low, so that it cannot be observed by commercial LEED systems because the broadening is hidden by the background. The high-resolution measurements, made up to now, have examined only the spot profile at the out-of-phase condition. Because the different origins of both broadenings can only be investigated by measuring the profile at many energies, especially close to the in-phase condition, the additional broadening may be erroneously associated with the broadening caused by steps.

Unfortunately, the origin of this second kind of scatterer is not yet clearly known. There may be some reasons for this phenomenon: (1) areas of impurities, especially oxygen and carbon, (2) areas where the lattice is disordered, (3) a combination of both origins (the lattice is disordered by the impurities), and (4) the edge atoms of terraces. Here we will discuss reasons why these inhomogeneities may be generated.

(1) One source of areas of different chemical composition may be that the oxide has not been removed totally and so there are residuals of the oxide on the surface of the bare silicon crystal. Also, residual gas may be adsorbed at the surface of the samples during the transfer of the samples into the UHV chamber. This hypothesis is supported by the observation that the broad shoulder vanishes after well annealing of the samples in the UHV chamber. Moreover, this explanation agrees with previous Auger measurements of transferred silicon crystals after removal of the oxide, which suggests a residual coverage about 0.3 monolayers.¹³ Hahn *et al.* have also reported that the background intensity increases after exposing the sample to the residual gas within the lock.

(2) The silicon crystal and its oxide are very different sorts of material. While the crystal is ordered well, the oxide is an amorphous material. During oxidation the silicon must release the well-ordered lattice of the crystal which may be the reason that areas of disturbed lattice come into existence.

(3) During oxidation, excess oxygen may diffuse through bulk silicon, especially close to the interface. Such oxygen may form oxide clusters or just lattice distortions over several atomic distances. Already here we want to draw your attention to that point, that all these inhomogeneities may nucleate preferentially at steps. Thus the inhomogeneities may be related to the structur-

al disorder of the interface, especially steps.

(4) Low-energy electrons are multiply scattered by the crystal. So there may be different scattering amplitudes of terrace atoms and edge atoms because their surroundings differ. This effect should most strongly influence the scattering by small islands. But we think that this explanation can be neglected because scattering amplitudes of edge and terrace atoms cannot differ for such a wide range of phases, as has been observed in our experiments.

The large half-width of the broad shoulder means that those distorted areas are fairly small, only 3-8 atomic distances in average. The geometric distribution of these areas points to a random process of generation without correlation. Since the geometric terrace distribution causes randomly distributed steps, these steps may be centers where domains of inhomogeneities nucleate preferentially. In big contrast to the step structure, the average domain size and the coverage with domains is drastically changed by annealing. So it is likely that during oxidation some defects at or close to the interface are generated, which to some extent may be annealed in nitrogen.

It is remarkable that annealing does not change the step distribution significantly. On the other hand, the unannealed wafer already shows an excellent interface: the step density is extremely low (only 2.3% of the surface atoms of a cross section are step atoms). The healing of the interface may occur mainly via the migration of single atoms or very small islands (whether these small islands consist of silicon and/or oxygen is not important here). Incorporating these small clusters into large islands, the length of not too small terraces is not changed drastically and a clear change of that part of the spot profiles is not expected. Unfortunately, the information about a variation of the small terraces is difficult to extract from the spot profile because the broad shoulder and the diffuse background hide the intensity mainly caused by small islands. But it may be possible that the change of the broad shoulder is a hint to the supposed diminishing of very small islands, since the small inhomogeneities may be related to terraces and islands of similar size.

The influence of the two types of defects (steps and inhomogeneities) on electrical properties so far can only be guessed.¹⁴ The reported effect on mobility may be due to both types of defects. It has been reported that interface state density, which is smaller than the step-atom density by orders of magnitude, varies also with the half-width. Here it is more likely that the inhomogeneities are the origin of the sites for fixed charges. For a clear conclusion, dedicated experiments are needed. It is, however, already shown that two different types of defects are present and measured quantitatively and separated experimentally, so that a direct correlation of both types of defects with electrical properties may be studied in detail.

ACKNOWLEDGMENTS

The silicon wafers and the oxidation have been kindly provided by Wacker Chemitronic, Burghausen. Support by the U.S. Army through its European Research Organization is acknowledged.

- ¹T. Ando, A. B. Fowler, and F. Stern, *Rev. Mod. Phys.* **54**, 437 (1982).
- ²A. Gold, *Phys. Rev. B* **32**, 4014 (1985).
- ³A. Gold, *Phys. Rev. Lett.* **54**, 1079 (1985).
- ⁴M. Henzler, *Appl. Phys. A* **34**, 205 (1984).
- ⁵M. Henzler, in *Festkörperprobleme (Advances in Solid State Physics)*, edited by H. J. Quisser (Pergamon, Braunschweig, 1987), Vol. 27, p. 185; in *Solid State Devices 1986*, IOP Conf. Proc. Ser. No. 82, edited by D. F. Moore (IOP, Bristol, 1987), p. 39.
- ⁶W. Braun and H. Kuhlenbeck, *Surf. Sci.* **180**, 279 (1987).
- ⁷F. J. Grunthaner, P. J. Grunthaner, R. P. Vasquez, B. F. Lewis, and J. Maserjian, *J. Vac. Sci. Technol.* **16**, 1443 (1979).
- ⁸F. J. Grunthaner, P. J. Grunthaner, M. H. Hecht, and Di Lawson, in *Insulating Films on Semiconductors*, edited by J. J. Simonne and J. Buxo (North-Holland, Amsterdam, 1986), p. 1.
- ⁹F. J. Grunthaner and P. J. Grunthaner, *Mater. Sci. Rep.* **1**, 65 (1986).
- ¹⁰S. M. Goodnick, R. G. Gann, J. R. Sites, D. K. Ferry, C. W. Wilmsen, D. Fathy, and O. L. Krivanek, *J. Vac. Sci. Technol. B* **1**, 803 (1983).
- ¹¹S. M. Goodnick, D. K. Ferry, C. W. Wilmsen, Z. Lilienthal, D. Fathy, and O. L. Krivanek, *Phys. Rev. B* **32**, 8171 (1985).
- ¹²O. L. Krivanek and J. H. Mazur, *Appl. Phys. Lett.* **37**, 392 (1980).
- ¹³P. O. Hahn and M. Henzler, *J. Appl. Phys.* **52**, 4122 (1981).
- ¹⁴P. O. Hahn and M. Henzler, *J. Vac. Sci. Technol. A* **2**, 574 (1984).
- ¹⁵M. Henzler, *Surf. Sci.* **152/153**, 963 (1985).
- ¹⁶R. M. Feenstra and G. S. Oehrlein, *Appl. Phys. Lett.* **47**, 97 (1985).
- ¹⁷R. A. Cowley and T. W. Ryan, *J. Phys. D* **20**, 61 (1987).
- ¹⁸M. G. Lagally, D. E. Savage, and M. C. Trinigides, in *Reflection High Energy Electron Diffraction and Reflection Electron Imaging of Surfaces*, edited by P. K. Larsen and P. I. Dobson (Plenum, New York, 1988), p. 139.
- ¹⁹J. Wollschläger, J. Falta, and M. Henzler (unpublished).
- ²⁰R. Altsinger, H. Busch, M. Horn, and M. Henzler, *Surf. Sci.* **200**, 235 (1988).
- ²¹M. Horn, U. Gotter, and M. Henzler, *J. Vac. Sci. Technol. B* **6**, 727 (1988).
- ²²H. Busch and M. Henzler, *Surf. Sci.* **167**, 534 (1986).
- ²³J. M. Pimbley and T. M. Lu, *J. Appl. Phys.* **55**, 182 (1984).
- ²⁴J. M. Pimbley and T. M. Lu, *J. Vac. Sci. Technol. A* **2**, 457 (1984).
- ²⁵P. Marienhoff, Ph.D. thesis, University of Hannover, 1988.
- ²⁶C. S. Lent and P. I. Cohen, *Surf. Sci.* **139**, 121 (1984).
- ²⁷M. Henzler and P. Marienhoff, *J. Vac. Sci. Technol. B* **2**, 346 (1984).